Microtubules are involved in anterior-posterior axis formation in *C. elegans* embryos

Miao-Chih Tsai[1,2] and Julie Ahringer[1,2]

[1]Gurdon Institute and [2]Department of Genetics, University of Cambridge, Cambridge CB2 1QN, England, UK

Microtubules deliver positional signals and are required for establishing polarity in many different organisms and cell types. In *Caenorhabditis elegans* embryos, posterior polarity is induced by an unknown centrosome-dependent signal. Whether microtubules are involved in this signaling process has been the subject of controversy. Although early studies supported such an involvement (O'Connell, K.F., K.N. Maxwell, and J.G. White. 2000. *Dev. Biol.* 222:55–70; Wallenfang, M.R., and G. Seydoux. 2000. *Nature.* 408:89–92; Hamill, D.R., A.F. Severson, J.C. Carter, and B. Bowerman. 2002. *Dev. Cell.* 3:673–684), recent work involving RNA interference knockdown of tubulin led to the conclusion that centrosomes induce polarity independently of microtubules (Cowan, C.R., and A.A. Hyman. 2004. *Nature.* 431:92–96; Sonneville, R., and P. Gonczy. 2004. *Development.* 131: 3527–3543). In this study, we investigate the consequences of tubulin knockdown on polarity signaling. We find that tubulin depletion delays polarity induction relative to wild type and that polarity only occurs when a small, late-growing microtubule aster is visible at the centrosome. We also show that the process of a normal meiosis produces a microtubule-dependent polarity signal and that the relative levels of anterior and posterior PAR (partitioning defective) polarity proteins influence the response to polarity signaling. Our results support a role for microtubules in the induction of embryonic polarity in *C. elegans*.

Introduction

In *Caenorhabditis elegans* embryos, the oocyte has no developmentally important polarity (Goldstein and Hird, 1996). After fertilization, the oocyte and sperm pronuclei are usually at opposite ends of the oblong embryo, and the oocyte pronucleus undergoes two meiotic divisions, extruding two polar bodies before polarity induction and mitosis (Oegema and Hyman, 2006). Posterior polarity is induced via an unknown centrosome-dependent signal brought in by the sperm (Goldstein and Hird, 1996; O'Connell et al., 2000; Sadler and Shakes, 2000; Wallenfang and Seydoux, 2000; Cowan and Hyman, 2004, 2006). This is thought to locally down-regulate actin contractility, leading to anterior movement of the anterior PAR (partitioning defective) polarity proteins PAR-3, PAR-6, and PKC-3 through the anterior contraction/movement of actin and nonmuscle myosin (Munro et al., 2004; Cowan and Hyman, 2007). Anterior PAR protein localization leads to the posterior cortical localization of PAR-2 (Cuenca et al., 2003). Establishment of the anterior and posterior cortical PAR domains is critical for all downstream polarized events (Gonczy and Rose, 2005).

Correspondence to Julie Ahringer: jaa@mole.bio.cam.ac.uk

Abbreviations used in this paper: dsRNA, double-stranded RNA; PAR, partitioning defective.

The online version of this article contains supplemental material.

Sperm in which centrosome maturation is defective, such as *spd-5* and *spd-2* mutants, often fail to induce posterior polarity (O'Connell et al., 2000; Hamill et al., 2002; Cowan and Hyman, 2004). The defect in centrosome maturation in *spd-5* and *spd-2* mutants causes a delay in the nucleation of microtubules, which led to the proposal that microtubules might be required for inducing posterior polarity (O'Connell et al., 2000; Hamill et al., 2002). Consistent with this idea, Wallenfang and Seydoux (2000) showed using a variety of mutant backgrounds that a persistent meiotic (acentrosomal) metaphase spindle can induce posterior polarity, with the posterior polarity protein PAR-2 being found near the arrested meiotic spindle at the presumptive anterior end rather than near the sperm pronucleus. This posterior polarity induction depends on microtubules, supporting the view that microtubules can provide polarity signaling and that centrosomes are not required (Wallenfang and Seydoux, 2000).

Recent studies have challenged a role for microtubules in polarity induction (Cowan and Hyman, 2004; Sonneville and Gonczy, 2004). After the knockdown of tubulin by RNAi or inhibition with the drug nocodazole, embryos can still establish embryonic polarity, with normal anterior and posterior PAR domains (Cowan and Hyman, 2004; Sonneville and Gonczy, 2004). These results, together with work showing that removal of

The Journal of Cell Biology, Vol. 179, No. 3, November 5, 2007 397–402
http://www.jcb.org/cgi/doi/10.1083/jcb.200708101

the centrosome by laser ablation leads to a failure of polarity induction, led to the conclusion that centrosomes induce polarity independently of microtubules (Cowan and Hyman, 2004; Sonneville and Gonczy, 2004). However, this model fails to explain how a meiotic spindle, which lacks centrosomes, can provide a polarity signal. In addition, although greatly reduced, tubulin is still detectable at the centrosome after RNAi of tubulin or nocodazole treatment (Hyman and White, 1987; Cowan and Hyman, 2004; Sonneville and Gonczy, 2004), leaving open the possibility that microtubules could be required for the posterior signal.

In this study, we explore the relationship between polarity signaling and PAR protein levels and carry out a detailed analysis of embryos in which tubulin levels are reduced. Our results strongly support a role for microtubules in polarity establishment.

Results and discussion

To identify embryonic polarity regulators, we tested a set of embryonic lethal genes by RNAi for inducing defects in the localization of GFP–PAR-2 in the one-celled embryo (unpublished data). One gene that showed a strong defect was *spd-5*, as previously reported (Hamill et al., 2002). SPD-5 is a centrosome component required for centrosome maturation and mitotic spindle assembly (Hamill et al., 2002).

We observed that most *spd-5(RNAi)* embryos showed reversed embryonic polarity, with GFP–PAR-2 near the meiotic polar bodies and opposite the sperm pronucleus (Fig. 1, E–H and Q). Both PAR-3 and the nonmuscle myosin NMY-2 also show a reversed distribution in *spd-5(RNAi)* embryos, suggesting that a normal process of polarity induction is occurring (Fig. 1 N and Fig. S1, available at http://www.jcb.org/cgi/content/full/jcb.200708101/DC1). Reversed embryonic polarity has previously been associated with mutants or RNAi knockdowns inducing a persistent or abnormal meiotic spindle (Wallenfang and Seydoux, 2000; Liu et al., 2004; Sonneville and Gonczy, 2004). However, no meiotic defects have been reported for *spd-5* mutants (Hamill et al., 2002). We confirmed that meiotic timing ($n = 5$) and polar body and spindle formation during meiotic divisions ($n = 6$) are normal in *spd-5(RNAi)* embryos. To test whether microtubules are responsible for the reversed posterior polarity signal, we used a β-tubulin mutant (Ellis et al., 2004) combined with RNAi to inhibit tubulin function in *spd-5(RNAi)* embryos (see Materials and methods). In such embryos, anteriorly localized PAR-2 was never detected (Table I, seventh column). In contrast, the total percentage of embryos that showed posterior PAR-2 in *spd-5(RNAi)* embryos was similar irrespective of the RNAi knockdown of tubulin (Table I, last column). These results show that a normal meiosis produces a microtubule-dependent signal that can induce posterior polarity.

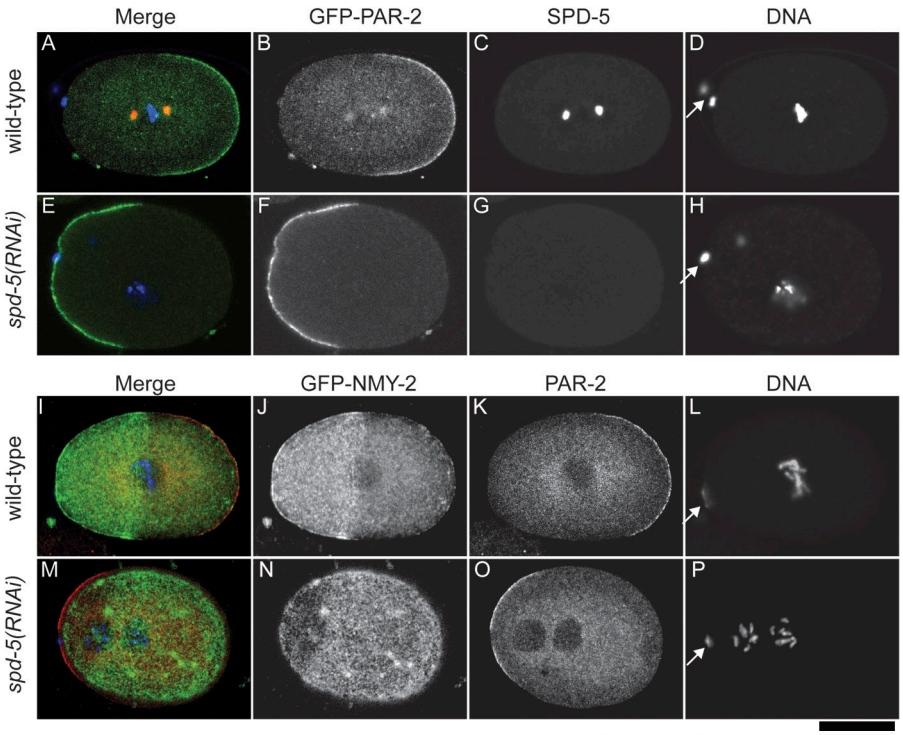

Q

Background	N	Cortical PAR-2 localization (%)			
		Anterior	Posterior	Both ends	None
wild-type	30	0	100	0	0
GFP-PAR-2; spd-5(RNAi)	73	80	3	8	10
spd-5(or213ts)	42	31	38	31	0
spd-5(or213ts); spd-5(RNAi)	55	52	24	22	2
GFP-PAR-6; spd-5(RNAi)	62	0	3	0	97

Figure 1. **Polarity reversal of *spd-5(RNAi)* embryos and dependence on relative PAR protein levels.** Wild-type (A–D and I–L) or *spd-5(RNAi)* embryos (E–H and M–P) carrying either GFP–PAR-2 (A–H) or GFP–NMY-2 (I–P). Embryos in A–H are stained for GFP–PAR-2, SPD-5, and DNA, and those in I–P are stained for GFP–NMY-2, PAR-2, and DNA as indicated. Embryos are oriented with polar bodies to the left (presumptive anterior), which are indicated by arrows in the DNA column. *spd-5(RNAi)* embryos show reversed polarity compared with wild type, which is indicated by reversed location of GFP–PAR-2 (F), PAR-2 (O), and GFP–NMY-2 (N) relative to polar bodies. (Q) Dependence of embryonic polarity on PAR protein levels. Wild-type or *spd-5(RNAi)* embryos of the indicated genotypes were scored for the location of cortical PAR-2; embryos were scored from mid-pronuclear migration to the end of the first mitosis. Bar, 25 μm.

Consistent with these data, wild-type embryos sometimes show a transient anterior cap of PAR-2 protein (Boyd et al., 1996). However, the timing of meiotic polarity induction differs from that of centrosome-dependent induction: reversed polarity in *spd-5(RNAi)* embryos occurs 10 min later than the initiation of normal posterior polarity in wild-type embryos (Fig. S2).

We observed a higher frequency of reversed polarity after RNAi of *spd-5* than in *spd-5(or213ts)* mutants (Fig. 1 Q, second and third rows; Hamill et al., 2002). A possible explanation for this is that *spd-5(or213ts)* embryos might have more SPD-5 activity because the mutant may not be a null allele. To test this idea, we used RNAi of *spd-5* to try to further reduce SPD-5 activity in *spd-5(or213ts)* embryos. Such embryos display a range of PAR-2 localization defects similar to those of *spd-5(or213ts)* mutants (Fig. 1 Q). This indicates that the difference in penetrance of the reversal of polarity is not caused by a difference in SPD-5 activity.

Our experiments assaying polarity defects of *spd-5(RNAi)* embryos were performed in a background harboring GFP–PAR-2 in addition to endogenous PAR-2 and, thus, have increased PAR-2 protein levels (Wallenfang and Seydoux, 2000; Hao et al., 2006). This raised the possibility that the difference in penetrance of reversed polarity could be caused by a difference in the relative levels of anterior and posterior PAR proteins. To investigate this hypothesis, we compared the localization of PAR-2 in *spd-5(RNAi)* embryos (1) carrying GFP–PAR-2, (2) carrying no PAR transgenes, and (3) in which the level of the anterior PAR protein PAR-6 was increased through a GFP–PAR-6 transgene (Cuenca et al., 2003). Strikingly, we found that the embryonic polarity phenotypes induced by *spd-5(RNAi)* in the three genotypes strongly differ: PAR-2 is exclusively at the anterior end of 80% of GFP–PAR-2 embryos, of 52% of embryos with wild-type PAR levels, and of 0% of GFP–PAR-6 embryos (Fig. 1 Q). Posterior polarity completely failed to be induced in 97% of these latter embryos, as they showed uniform GFP–PAR-6 and no PAR-2 on the cortex (Fig. 1 Q and not depicted). Because the polarity signaling events in the three genotypes are expected to be equivalent, these results suggest that the ability of a signal to induce polarity depends on the relative levels of the PAR proteins.

The similarity in the reversed polarity induced by a meiotic microtubule-dependent (acentrosomal) signal and a sperm centrosome-dependent signal prompted us to reexamine a role for microtubules in posterior polarity induction. We used RNAi to simultaneously deplete α and β tubulins (hereafter referred to as *tubulin(RNAi)*; see Materials and methods). Extended RNAi of hermaphrodites led to maternal sterility, indicating that embryos completely devoid of tubulin cannot be produced (see Materials and methods). To achieve as strong a depletion as possible, we analyzed the embryos produced in a time window when 50–90% of double-stranded RNA (dsRNA)–injected hermaphrodites were sterile. To assess the effects of tubulin knockdown at different early embryonic stages, we carefully classified embryo age using the state of DNA condensation: stage 1, meiosis; stage 2, no DNA condensation; stage 3, initiation of DNA condensation; stage 4, intermediate DNA condensation; and stage 5, full DNA condensation (see Fig. 2 for staging criteria). We then compared the pattern of tubulin staining in wild-type and *tubulin(RNAi)* embryos.

Wild-type embryos display a strong cortical network of microtubules at all of these stages (Fig. 2, A–E). At stage 1 (meiosis), microtubules are additionally visible in the meiotic spindle (Fig. 2 A). In stage 2, only the cortical network is observed (Fig. 2 B). In stage 3, most (92%) embryos have apparent centrosomal asters, which are found in 100% of stage 4 and stage 5 embryos (Fig. 2, C–E and K). In *tubulin(RNAi)* embryos, tubulin immunoreactivity is strongly diminished at all stages (Fig. 2, F–J). During meiotic stages, embryos lack cortical microtubules but show a small concentration of tubulin around the maternal DNA (Fig. 2 F). At stage 2, a weak network of cortical tubulin fibers is visible (Fig. 2 G). In contrast to wild type, only 22% of stage 3 and 34% of stage 4 *tubulin(RNAi)* embryos show a concentration of tubulin staining at the centrosome, with the remainder having weak cortical microtubules (Fig. 2, H, I, and K). At stage 5, 89% have detectable microtubules at the centrosome. This analysis shows that after strong tubulin knockdown, a small centrosomal microtubule aster eventually forms, but at a later time than in wild-type embryos.

To confirm that tubulin knockdown does not impair the accumulation of other centrosomal proteins, we examined two centrosome markers in *tubulin(RNAi)* embryos. We found that the centrosomal accumulation of SPD-5 (Hamill et al., 2002) and TAC-1 (Bellanger and Gonczy, 2003; Le Bot et al., 2003; Srayko et al., 2003) are normal in *tubulin(RNAi)* embryos ($n = 13$ and $n = 8$, respectively; Fig. 3 and not depicted).

We then compared polarity induction in wild-type and *tubulin(RNAi)* embryos. In wild-type embryos, polarity is initiated

Table I. **Anterior localization of PAR-2 in *spd-5(RNAi)* embryos is microtubule dependent**

Genetic background		PAR-2 location					
	n	Anterior only	Posterior only	Both ends	None	Anterior total	Posterior total
		%	%	%	%	%	%
N2 (wild type)	30	0	100	0	0	0	100
tbb-2(or362ts)	27	0	93	0	7	0	93
tbb-2(or362ts); tubulin(RNAi)	44	0	93	0	7	0	93
tbb-2(or362ts); spd-5(RNAi)	80	18	42	12	28	30	54
tbb-2(or362ts); spd-5(RNAi); tubulin(RNAi)	30	0	53	0	47	0	53

Embryos of the indicated genotypes were scored for the location of PAR-2 as indicated. Anterior total is the sum of the Anterior only and Both ends columns. Posterior total is the sum of the Posterior only and Both ends columns. Anterior PAR-2 induced by *spd-5(RNAi)* (30%; second to last row) is abolished by RNAi of tubulin (0%; last row). Posterior PAR-2 (last column) is unchanged (54% vs. 53%).

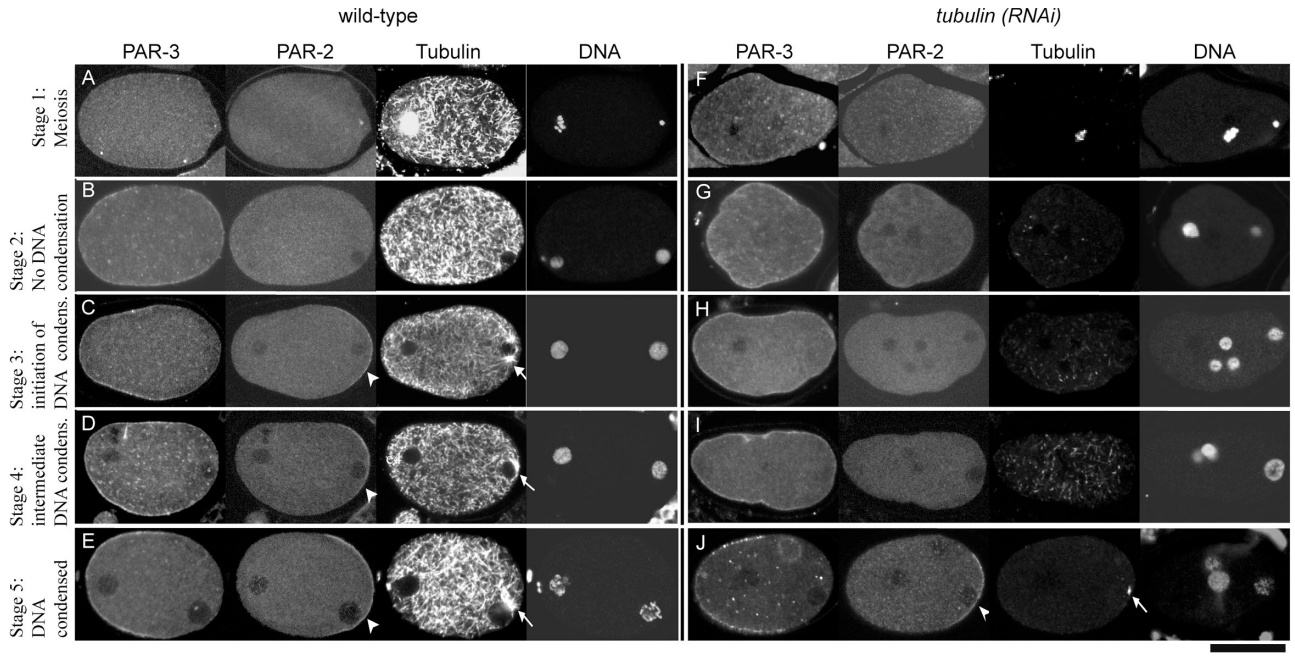

K

	Stage 2: no DNA condensation		n	Stage 3: initiation of DNA condensation				n	Stage 4: intermediate DNA condensation				n	Stage 5: DNA condensed				n
	Polarized	-		-	-	+	+		-	-	+	+		-	-	+	+	
	Asters	-		-	+	-	++		-	+	-	++		-	+	-	++	
wild-type		100%	22	8%	23%	0%	69%	26	0%	0%	0%	100%	9	0%	0%	0%	100%	27
tubulin(RNAi)		100%	7	78%	11%	0%	11%	9	67%	17%	0%	17%	5	11%	5%	0%	84%	19

Figure 2. **Concurrent delay in microtubule aster growth and polarity induction caused by tubulin knockdown.** Series of wild-type (A–E) and *tubulin(RNAi)* (F–J) embryos stained for PAR-3, PAR-2, tubulin, and DNA; all embryos carry the *zuEx69* (par-6–GFP–PAR-6) transgene. Arrowheads in the PAR-2 columns indicate cortical PAR-2, and arrows in the tubulin columns indicate microtubule asters. Embryo age staged by the state of DNA condensation is labeled at the left. Staging was as follows: stage 1, meiosis; stage 2, no DNA condensation (uniform DAPI staining); stage 3, initiation of DNA condensation (small scattered areas of bright DAPI staining and general nuclear staining); stage 4, intermediate DNA condensation (strings of bright DAPI staining and general nuclear staining); and stage 5, full DNA condensation (strings of bright DAPI staining with dark nuclear background). (K) Quantification of staining results. Each embryo was scored for stage, presence of a microtubule aster, and evidence of polarity (scored by the presence of asymmetric PAR domains). Aster sizes were classified as small (+) or large (++). For wild type, + indicates a small concentration of tubulin at the centrosome, and ++ indicates that microtubules emanating from the centrosome were detectable. For *tubulin(RNAi)*, + indicates a small dot of tubulin at the centrosome, and ++ indicates a small aster, as in J. The percentage of embryos of the indicated phenotype and the number of embryos in the indicated class are shown. Bar, 30 μm.

at stage 3 (initiation of DNA condensation; Fig. 1 K). At this stage, we observed that 69% of such embryos had posterior PAR-2, all of which had visible asters; a further 23% had lower but detectable levels of tubulin at the centrosome but no obvious cortical PAR-2 (Fig. 2, C and K). At stage 4 (intermediate DNA condensation) and stage 5 (full DNA condensation), all wild-type embryos were polarized and had robust asters (Fig. 2, D, E, and K). These results show that similar to a previous study (Cuenca et al., 2003), the initiation of polarity is strongly correlated with growth of the sperm aster.

We found that polarity induction in *tubulin(RNAi)* embryos was delayed relative to wild type and was only apparent in embryos with centrosomal asters. Whereas the majority of wild-type embryos are polarized at stage 3, only 11% of *tubulin(RNAi)* embryos are polarized at this stage (Fig. 2, H and K). Similarly, at stage 4, when all wild-type embryos are polarized, only 17% of *tubulin(RNAi)* embryos are polarized (Fig. 2, I and K). Importantly, although only a minority of stage 3 and stage 4 *tubulin(RNAi)* embryos have asters (22% and 34%, respectively), all of the polarized *tubulin(RNAi)* embryos had visible asters (Fig. 2 K). At stage 5, 11% of *tubulin(RNAi)* embryos still lacked asters, and these were not polarized (Fig. 2 K). Therefore, there is a tight correlation between the time of polarity induction and microtubule aster growth in both wild-type embryos and *tubulin(RNAi)* embryos. Because centrosomal microtubule growth is delayed in the context of a normal centrosome in *tubulin(RNAi)* embryos, these results strongly argue that microtubules are required for polarity induction.

Previous work demonstrated that the polarity signal is dependent on the centrosome and that centrosome maturation is critical for the signal (O'Connell et al., 2000; Hamill et al., 2002; Cowan and Hyman, 2004). Mutants that impair centrosome maturation fail to polarize (O'Connell et al., 2000; Hamill et al., 2002). Regulation of centrosome maturation timing by cyclin E (CYE-1) is also important, as RNAi of *cye-1* delays maturation and prevents polarity induction (Cowan and Hyman, 2006).

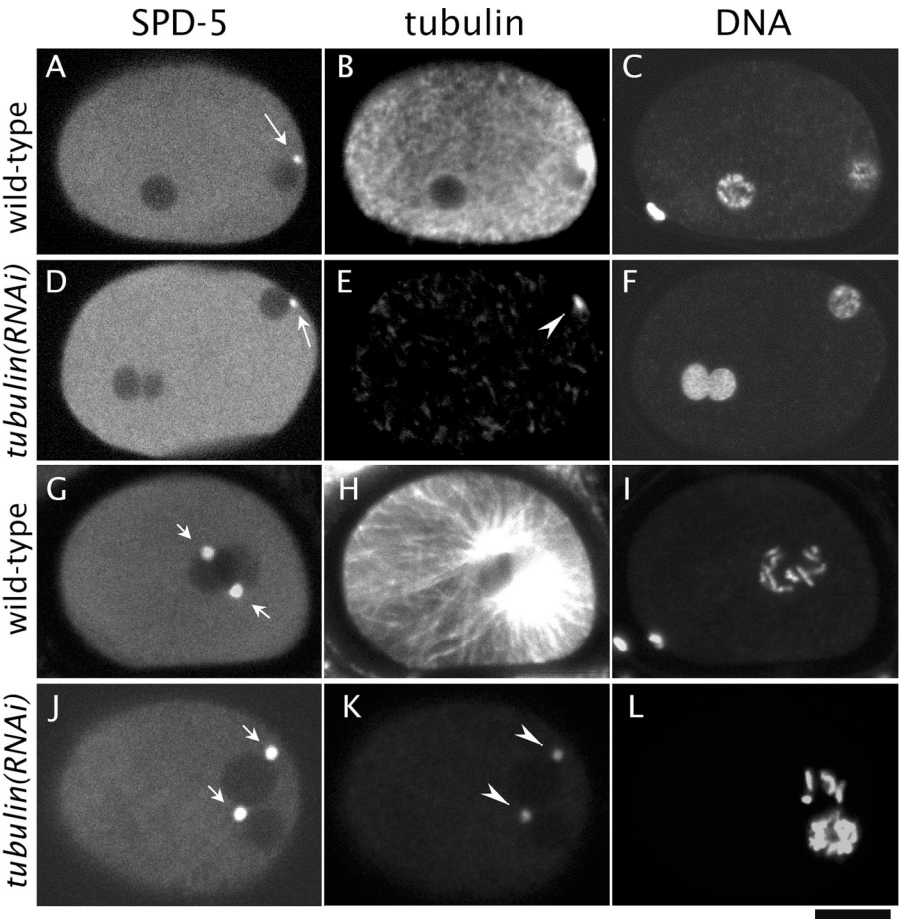

Figure 3. **RNAi knockdown of tubulin does not impair SPD-5 accumulation at the centrosome.** Wild-type (A–C and G–I) and *tubulin(RNAi)* embryos (D–F and J–L) stained for SPD-5, tubulin, and DNA. *tubulin(RNAi)* embryos show the normal accumulation of SPD-5 at early and late stage one-cell embryos (D and J; $n = 13$). Arrows and arrowheads point to centrosomes. Bar, 13 μm.

Our work supports the view that the delay in microtubule growth caused by centrosome maturation defects in these mutants is responsible for the impairment in polarity induction.

Microtubule involvement in both the centrosome-dependent signal and a meiosis-dependent signal suggests that both processes may use a similar signaling mechanism. However, the timing of these signals appears to be different. We found that the meiotic signal induces PAR polarity ~13 min after the completion of meiotic divisions and 10 min later than centrosome-dependent posterior polarity (Fig. S2). Therefore, it seems unlikely that it is the meiotic spindle itself that is delivering a signal. The meiotic divisions produce two polar bodies that have associated midbodies, or spindle remnants where they are attached to the embryo. Because these spindle remnants contain microtubules, one possibility is that this is the source of the meiotic polarity signal. The time of meiotic signaling is coincident with rapid mitotic centrosomal microtubule growth, which might induce growth/activity of the spindle remnant ends.

What could be the nature of the microtubule-dependent signal? It is surprising that components have not yet been found given the extensive genetic and RNAi screening that has been conducted for cell polarity genes. A possible reason for this is that polarity induction might involve partially redundant signaling pathways, which are commonly seen in other processes. Good candidates for involvement are microtubule plus end–binding proteins, many of which either regulate microtubule dynamics or influence cortical processes (Akhmanova et al., 2005). Identifying the signaling and receiving factors is the most crucial future task for understanding the mechanism of polarity induction.

Materials and methods

Strains

The following strains were used, culturing by standard methods (Brenner, 1974): wild-type Bristol N2, JJ1473: *zuIs45* [*nmy-2*–NMY-2–GFP; *unc-119(+)*] (Munro et al., 2004), zuEx69 [*par-6*–GFP–PAR-6] (Nance et al., 2003), JH1512: *axIs1137* [*rol-6(d); pie-1*–GFP–PAR-6] (Cuenca et al., 2003), *tbb-2(or362ts)* (Ellis et al., 2004), KK866 *itIs153* [pie-1–PAR-2–GFP] (Wallenfang and Seydoux, 2000), EU856: *spd-5(or213)* (Hamill et al., 2002), JA1390 *itIs153* [*pie-1*–PAR-2–GFP, *unc-119(+)*], and *ruIs57* [*pie-1*–β-tubulin–GFP), *unc-119(+)*] (Wallenfang and Seydoux, 2000; Praitis et al., 2001).

RNAi

Synthesis of dsRNA and RNAi was performed by injection as described previously (Ahringer, 2006) using RNAi feeding clones from Fraser et al. (2000) and Kamath et al. (2003) as templates for RNAi synthesis (sjj_F56A3.4 for *spd-5*, sjj_C47B2.3 for *tba-2*, and sjj_C36E8.5 for *tbb-2*). RNAi of α- and β-tubulin genes was performed by combining dsRNA with both *tba-2* and *tbb-2*. Because of the high level of sequence identity among tubulin genes, *tba-2* dsRNA will additionally target *tba-1*, and *tbb-2* dsRNA will target *tba-1*. In all *tubulin(RNAi)* experiments, *tba-1* and *tbb-2* dsRNAs were coinjected, and experiments were conducted at 25°C. 50–90% of *tubulin(RNAi)* hermaphrodites are sterile at 22–30 h after injection; at 40 h, all hermaphrodites are sterile even though sperm are still present. *spd-5(RNAi)* in Fig. 1 was performed at 25°C, and embryos were dissected 30 h after injection. *tubulin(RNAi)* experiments were performed for 22–30 h at 25°C.

Immunofluorescence

Antibody staining was performed as described previously (Andrews and Ahringer, 2007). Antibodies used were rabbit anti–SPD-5 (Hamill et al., 2002), rat anti–PAR-3 (Dong et al., 2007), rabbit anti–PAR-2 (Dong et al., 2007), rabbit anti–TAC-1 (Le Bot et al., 2003), mouse antitubulin (clone DM1 A1; Sigma-Aldrich), and chicken anti-GFP (Chemicon). Secondary antibodies were purchased from Jackson ImmunoResearch Laboratories. Confocal images were taken on either an LSM 510 Meta microscope (Carl Zeiss MicroImaging, Inc.) or a Radiance instrument (Bio-Rad Laboratories). Wild-type and RNAi experiments were conducted in pairs, and images were taken using the same settings.

Video microscopy

For live recordings in Fig. S2, *itIs153* [*pie-1*–PAR-2–GFP] and *ruIs57* [pie-1–β-tubulin–GFP] were mounted in egg buffer (118 mM NaCl, 40 mM KCl, 3 mM $CaCl_2$, 3 mM $MgCl_2$, and 5 mM Hepes, pH 7.2) on 18 × 18-mm coverslips coated with 0.3% poly-lysine (Sigma-Aldrich), and the coverslips were inverted onto 3% agar pads and sealed with petroleum jelly. Paired images were taken every 10 s using a 63× lens on a fluorescence microscope (Axioplan 2; Carl Zeiss MicroImaging, Inc.) and 3DM software (Improvision).

Online supplemental material

Fig. S1 shows that *spd-5(RNAi)* embryos show a reversal of anterior and posterior PAR domains. Fig. S2 shows that reversed PAR-2 polarity in *spd-5(RNAi)* embryos is delayed relative to wild-type PAR-2 polarity. Online supplemental material is available at http://www.jcb.org/cgi/content/full/jcb.200708101/DC1.

We thank B. Bowerman, E. Munro, J. Nance, and G. Seydoux for strains and reagents and D. Rivers, I. Latorre, and D. St. Johnston for comments on the manuscript. We also thank Y. Dong for excellent technical assistance. Some strains used in this work were provided by the *Caenorhabditis* Genetics Center, which is funded by the National Institutes of Health National Center for Research Resources.

J. Ahringer is supported by a Wellcome Trust Senior Research Fellowship (grant 054523).

Submitted: 14 August 2007
Accepted: 1 October 2007

References

Ahringer, J. 2006. Reverse genetics. *In* WormBook. The *C. elegans* Research Community, editors. doi:10.1895/wormbook.1.47.1. http://www.wormbook.org.

Akhmanova, A., A.L. Mausset-Bonnefont, W. van Cappellen, N. Keijzer, C.C. Hoogenraad, T. Stepanova, K. Drabek, J. van der Wees, M. Mommaas, J. Onderwater, et al. 2005. The microtubule plus-end-tracking protein CLIP-170 associates with the spermatid manchette and is essential for spermatogenesis. *Genes Dev.* 19:2501–2515.

Andrews, R., and J. Ahringer. 2007. Asymmetry of early endosome distribution in *C. elegans* embryos. *PLoS ONE*. doi:10.1371/journal.pone.0000493.

Bellanger, J.M., and P. Gonczy. 2003. TAC-1 and ZYG-9 form a complex that promotes microtubule assembly in *C. elegans* embryos. *Curr. Biol.* 13:1488–1498.

Boyd, L., S. Guo, D. Levitan, D.T. Stinchcomb, and K.J. Kemphues. 1996. PAR-2 is asymmetrically distributed and promotes association of P granules and PAR-1 with the cortex in *C. elegans* embryos. *Development*. 122:3075–3084.

Brenner, S. 1974. The genetics of *Caenorhabditis elegans*. *Genetics*. 77:71–94.

Cowan, C.R., and A.A. Hyman. 2004. Centrosomes direct cell polarity independently of microtubule assembly in *C. elegans* embryos. *Nature*. 431:92–96.

Cowan, C.R., and A.A. Hyman. 2006. Cyclin E-Cdk2 temporally regulates centrosome assembly and establishment of polarity in *Caenorhabditis elegans* embryos. *Nat. Cell Biol.* 8:1441–1447.

Cowan, C.R., and A.A. Hyman. 2007. Acto-myosin reorganization and PAR polarity in *C. elegans*. *Development*. 134:1035–1043.

Cuenca, A.A., A. Schetter, D. Aceto, K. Kemphues, and G. Seydoux. 2003. Polarization of the *C. elegans* zygote proceeds via distinct establishment and maintenance phases. *Development*. 130:1255–1265.

Dong, Y., A. Bogdanova, B. Habermann, W. Zachariae, and J. Ahringer. 2007. Identification of the *C. elegans* anaphase promoting complex subunit Cdc26 by phenotypic profiling and functional rescue in yeast. *BMC Dev. Biol.* 7:19.

Ellis, G.C., J.B. Phillips, S. O'Rourke, R. Lyczak, and B. Bowerman. 2004. Maternally expressed and partially redundant beta-tubulins in *Caenorhabditis elegans* are autoregulated. *J. Cell Sci.* 117:457–464.

Fraser, A.G., R.S. Kamath, P. Zipperlen, M. Martinez-Campos, M. Sohrmann, and J. Ahringer. 2000. Functional genomic analysis of *C. elegans* chromosome I by systematic RNA interference. *Nature*. 408:325–330.

Goldstein, B., and S.N. Hird. 1996. Specification of the anteroposterior axis in *Caenorhabditis elegans*. *Development*. 122:1467–1474.

Gonczy, P., and L.S. Rose. 2005. Asymmetric cell division and axis formation in the embryo. *In* WormBook. The *C. elegans* Research Community, editors. doi:10.1895/wormbook.1.30.1. http://www.wormbook.org.

Hamill, D.R., A.F. Severson, J.C. Carter, and B. Bowerman. 2002. Centrosome maturation and mitotic spindle assembly in *C. elegans* require SPD-5, a protein with multiple coiled-coil domains. *Dev. Cell*. 3:673–684.

Hao, Y., L. Boyd, and G. Seydoux. 2006. Stabilization of cell polarity by the *C. elegans* RING protein PAR-2. *Dev. Cell*. 10:199–208.

Hyman, A.A., and J.G. White. 1987. Determination of cell division axes in the early embryogenesis of *Caenorhabditis elegans*. *J. Cell Biol.* 105:2123–2135.

Kamath, R.S., A.G. Fraser, Y. Dong, G. Poulin, R. Durbin, M. Gotta, A. Kanapin, N. Le Bot, S. Moreno, M. Sohrmann, et al. 2003. Systematic functional analysis of the *Caenorhabditis elegans* genome using RNAi. *Nature*. 421:231–237.

Le Bot, N., M.C. Tsai, R.K. Andrews, and J. Ahringer. 2003. TAC-1, a regulator of microtubule length in the *C. elegans* embryo. *Curr. Biol.* 13:1499–1505.

Liu, J., S. Vasudevan, and E.T. Kipreos. 2004. CUL-2 and ZYG-11 promote meiotic anaphase II and the proper placement of the anterior-posterior axis in *C. elegans*. *Development*. 131:3513–3525.

Munro, E., J. Nance, and J.R. Priess. 2004. Cortical flows powered by asymmetrical contraction transport PAR proteins to establish and maintain anterior-posterior polarity in the early *C. elegans* embryo. *Dev. Cell*. 7:413–424.

Nance, J., E.M. Munro, and J.R. Priess. 2003. *C. elegans* PAR-3 and PAR-6 are required for apicobasal asymmetries associated with cell adhesion and gastrulation. *Development*. 130:5339–5350.

O'Connell, K.F., K.N. Maxwell, and J.G. White. 2000. The spd-2 gene is required for polarization of the anteroposterior axis and formation of the sperm asters in the *Caenorhabditis elegans* zygote. *Dev. Biol.* 222:55–70.

Oegema, K., and A.A. Hyman. 2006. Cell division. *In* WormBook. The *C. elegans* Research Community, editors. doi:10.1895/wormbook.1.72.1. http://www.wormbook.org.

Praitis, V., E. Casey, D. Collar, and J. Austin. 2001. Creation of low-copy integrated transgenic lines in *Caenorhabditis elegans*. *Genetics*. 157:1217–1226.

Sadler, P.L., and D.C. Shakes. 2000. Anucleate *Caenorhabditis elegans* sperm can crawl, fertilize oocytes and direct anterior-posterior polarization of the 1-cell embryo. *Development*. 127:355–366.

Sonneville, R., and P. Gonczy. 2004. Zyg-11 and cul-2 regulate progression through meiosis II and polarity establishment in *C. elegans*. *Development*. 131:3527–3543.

Srayko, M., S. Quintin, A. Schwager, and A.A. Hyman. 2003. *Caenorhabditis elegans* TAC-1 and ZYG-9 form a complex that is essential for long astral and spindle microtubules. *Curr. Biol.* 13:1506–1511.

Wallenfang, M.R., and G. Seydoux. 2000. Polarization of the anterior-posterior axis of *C. elegans* is a microtubule-directed process. *Nature*. 408:89–92.